Eur. Phys. J. Special Topics **226**, 1867–1881 (2017)

DOI: 10.1140/epjst/e2017-70007-1

THE EUROPEAN PHYSICAL JOURNAL SPECIAL TOPICS

Regular Article

Multiple scroll wave chimera states

Volodymyr Maistrenko[1,a], Oleksandr Sudakov[1,2], Oleksiy Osiv[1], and Yuri Maistrenko[1,3]

[1] Scientific Center for Medical and Biotechnical Research, NAS of Ukraine, Volodymyrska Str. 54, 01030 Kyiv, Ukraine
[2] Taras Shevchenko National University of Kyiv, Volodymyrska Str. 60, 01030 Kyiv, Ukraine
[3] Institute of Mathematics, NAS of Ukraine, Tereshchenkivska Str. 3, 01030 Kyiv, Ukraine

Received 29 January 2017 / Received in final form 13 March 2017
Published online 21 June 2017

Abstract. We report the appearance of three-dimensional (3D) multiheaded chimera states that display cascades of self-organized spatiotemporal patterns of coexisting coherence and incoherence. We demonstrate that the number of incoherent chimera domains can grow additively under appropriate variations of the system parameters generating thereby head-adding cascades of the scroll wave chimeras. The phenomenon is derived for the Kuramoto model of N^3 identical phase oscillators placed in the unit 3D cube with periodic boundary conditions, parameters being the coupling radius r and phase lag α. To obtain the multiheaded chimeras, we perform the so-called 'cloning procedure' as follows: choose a sample single-headed 3D chimera state, make appropriate scale transformation, and put some number of copies of them into the unit cube. After that, start numerical simulations with slightly perturbed initial conditions and continue them for a sufficiently long time to confirm or reject the state existence and stability. In this way it is found, that multiple scroll wave chimeras including those with incoherent rolls, Hopf links and trefoil knots admit this sort of multiheaded regeneration. On the other hand, multiple 3D chimeras without spiral rotations, like coherent and incoherent balls, tubes, crosses, and layers appear to be unstable and are destroyed rather fast even for arbitrarily small initial perturbations.

1 Introduction

Chimera states represent one of the most fascinating discoveries of modern nonlinear science at the border of the network and chaos theories. It has been found that networks of identical oscillators with non-local coupling can demonstrate robust coexistence of coherence and incoherence, such that a part of the network oscillators are synchronized but the others exhibit desynchronized and often chaotic behavior. First, the chimera phenomenon was described in 2002 for the *one-dimensional* complex Ginzburg-Landau equation and its phase approximation, the Kuramoto model [1].

[a] e-mail: maistren@nas.gov.ua

This paper stimulated the study [2] two years later. Both have opened a substantially new direction in the research of oscillatory networks. See recent review papers on the topic [3,4].

At about the same time, this novel approach was extended to *two-dimensional* networks of oscillators. Spiral waves with a randomized core were identified for a class of three-component reaction-diffusion systems in the plane and for the two-dimensional Ginzburg-Landau equation as well as for the corresponding non-locally coupled Kuramoto model [5–7]. They constitute a new class of chimera states, called the spiral wave chimeras [8]. This kind of spatio-temporal behavior is different from the oscillating 2D chimeras in which the coherent region only oscillates but does not spiral around the incoherence. The oscillating chimeras which are the natural counterparts of the 1D chimeras have been obtained in the form of stripes and spots, both coherent and incoherent [9,10] and also twisted states [11]. An interesting observation is that chimeras of both classes, oscillating and spiraling, emerge in opposite corners of the system parameter space and thus cannot co-exist [9].

The first evidence of chimera states in *three-dimensions* was reported two years ago in [12] for the Kuramoto model of coupled phase oscillators in three-dimensional (3D) grid topology

$$\dot{\varphi}_{ijk} = \omega + \frac{K}{N_P} \sum_{(i',j',k') \in B_P(i,j,k)} \sin(\varphi_{i'j'k'} - \varphi_{ijk} - \alpha), \tag{1}$$

where φ_{ijk} are phase variables, and indexes i, j, k are periodic mod N. The coupling is assumed long-ranged and isotropic: each oscillator φ_{ijk} is coupled with equal strength K to all its N_P nearest neighbors $\varphi_{i'j'k'}$ within a ball of radius P, i.e., to those falling in the neighborhood

$$B_P(i,j,k) := \{(i',j',k'):(i'-i)^2 + (j'-j)^2 + (k'-k)^2 \leq P^2\},$$

where the distances are calculated taking into account the periodic boundary conditions of the network. The phase lag parameter α is assumed to belong to the attractive coupling range from 0 to $\pi/2$. The second control parameter, coupling radius $r = P/N$ varies from $1/N$ (local coupling) to 0.5 (close to global coupling). Without loss of generality, we put in equation (1) $\omega = 0$ and $K = 1$.

In [12], two principal families of 3D chimera states were obtained for equation (1): type I – oscillating chimeras, i.e., those without spiraling of the coherent region, and type II – spirally rotating chimeras, called *scroll wave chimeras*. Examples of the first class are coherent and incoherent balls, tubes, crosses, and layers in incoherent or coherent surrounding, respectively; the second class includes incoherent rolls of different modality and space disposition in a spiraling rotating coherent surrounding. As it is illustrated in Figure 1, parameter regions for chimeras of both classes (type I) and (type II) do not intersect, while there is a huge multistability inside each of the classes.

Recently, two new kinds of the scroll wave chimeras, Hopf link and trefoil, with linked and knotted incoherent regions ("swelling" filaments) were detected in [13]. Our simulations confirm their existence in an ellipse-like parameter region which can be seen inside the type II chimera regions in Figure 1 (delineated in black). Furthermore, there exist in equation (1) scroll wave chimeras in the form of chains with one and two links. Parameter regions for one- and two-link chain chimeras are shown in Figure 1 too (delineated in red and brown). In the R^3-cube they look broken. However, they are indeed closed when considering them on the T^3-torus (which is topologically equivalent to the R^3-cube in the case of periodic boundary conditions). Note that all chimera patterns presented in Figure 1 are obtained with randomly chosen initial conditions.

In the present paper, we study the appearance of multiheaded 3D chimera states built up on a base of the single- and low-headed states exhibited in Figure 1. Similar

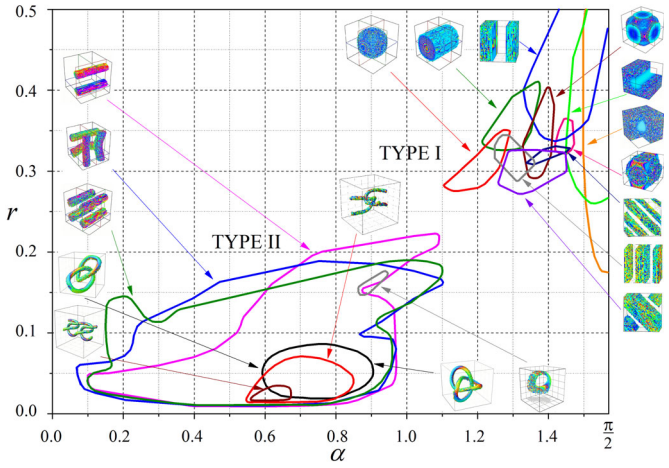

Fig. 1. Parameter regions of 3D chimera states for equation (1). Regions for type I oscillating and type II scroll wave chimeras appear in opposite corners of the parameter space. Snapshots of the states are shown in inserts. $r = P/N$. $N = 100$.

to the 1D case [14], we design cascades of multiple 3D chimeras with an increasing number of incoherent regions and obtain parameter regions for their existence. To illuminate the multiheaded scroll wave appearances, we apply the so-called "cloning procedure" as follows: glue a few copies of a chosen 3D chimera state, rescale them and stow them in the unit cube with periodic boundary conditions. Afterwards start a simulation with the constructed multiheaded initial conditions perturbed slightly to prevent the symmetry capturing effect.

We show, with the use of massive numerical simulations, that the cloning procedure perfectly works for the type II, i.e., scroll wave chimeras including rolls, Hopf links, and trefoils. The calculations were performed, as a rule, up to $t = 10^4$ time units which corresponds to approximately 100 periods of the spiral rotations in the patterns.

On the other hand, it fails for for the type I oscillating chimeras, as well as chains. They disappear in the processes of simulation as soon as the symmetry imposed is violated. Cascades of the roll-type scroll wave chimeras with even numbers of incoherent rolls are constructed in Section 2. Hopf link and trefoil cascades are obtained in Section 3. "Hybrid chimeras" including different combinations of trefoil, Hopf links and parallel rolls are illustrated in Section 4. Examples of the multiheaded scroll wave dynamics are demonstrated by videos at `http://chimera3d.biomed.kiev.ua/multiheaded`.

Numerical simulations were performed on the base of Runge-Kutta solver DOPRI5 that was integrated into the software for large nonlinear dynamical networks [15], allowing for parallelized simulations with different sets of parameters and initial conditions. The simulations were performed on the computer cluster "CHIMERA", `http://nll.biomed.kiev.ua/cluster`, and the Ukrainian Grid Infrastructure providing distributed cluster resources and the parallel software [16].

2 Cascades of scroll wave chimeras with multiple incoherent rolls

Scroll waves with parallel incoherent rolls represent one of the characteristic examples of the chimera states in three-dimensions. In [12], 2- and 4-rolled chimeras of this type were obtained, they exist in wide regions of the (α, r)-parameter space shown in

Figure 1. Due to the periodic boundary conditions they can be considered as scroll rings with incoherent cores ("swelling" filaments) on the T^3-torus. The microscopic dynamics inside the chimera rolls is chaotic while, on the large-scale, the rolls themselves are practically stationary, i.e., not moving in a significant manner. This can be seen in the supplementary videos of [12], also at `http://chimera3d.biomed.kiev.ua/high-resolution` (files fig5(a)hq-video.mkv, fig5(b)hq-video.mkv); as well as for 16, 64 parallel and 16 crossed rolls in `http://chimera3d.biomed.kiev.ua/multiheaded/rolls/`.

In Figure 2, a cascade of scroll wave chimeras with pair-multiple incoherent parallel rolls is presented. The number of rolls increases additively from 2 (Fig. 2a) to 16 (Fig. 2h). In addition, a 64-rolled chimera is shown in (Fig. 2i). The chimera rolls in Figure 2 are symmetrically located in the unit cube. However, the large-scale symmetry can be violated when other initial conditions are chosen. Note also that microscopic chaotic dynamics inside the rolls differ for different rolls of the same state, which is illustrated by the cross-sections shown below the 3D plots in Figure 2.

Regions for existence of the parallel rolled chimeras in the (α, r)-parameter plane are shown in Figure 3. They lie at intermediate phase shifts α between 0.1 and 0.95, and at small coupling radius $r < 0.12$ including the minimal possible $r = 0.01$ when only 6 nearest neighbors are connected to each oscillator ($N = 100$). Thus, the multiple rolled chimeras exist in the model (1) not only for non-local but also for the local coupling scheme. Based on this, we assume that such states should exist also in the limiting PDE case $N \to \infty, r \to 0$. If so, the PDE obtained by this a way could be a rich source for multiple scroll waves (multiple scroll rings when written in the circular coordinates). Our simulations confirm that chimeras illustrated in Figure 2 are robust 3D patterns as they survive for long integration times of thousands of rotating periods. Further study in this direction would be interesting from both theoretical and practical points of view; e.g., in medicine as prospective models of spiral patterns formed on heart tissue during ventricular tachycardia and fibrillation (see [3,12] and references therein).

To obtain the multi-rolled scroll wave chimeras we used the so-called 'cloning procedure' as follows. First, take some number of 2- or 4-rolled parallel chimeras (previously obtained in [12]). Rescale them in an appropriate way and fill the unit cube with them. Afterwards, start calculations with these specially prepared initial conditions slightly perturb to prevent the symmetry capturing effect. Doing so, there is no guarantee that the resulting state will be of the form as assigned, i.e., with the initially chosen number of rolls. We often had to repeat the procedure trying different variants of the number and type of initial 'chimera clones', as well as varying system parameters. Proceeding in such a way, after some number of trials the desired chimera pattern was usually obtained.

Among other variants of the cloning procedure, there is one reliable approach always giving the chimera state we are looking for. This is in the case when just 8 identical parallel chimeras are taken as samples and placed, after rescaling, in the unit cube. Then, a fourfold rolled chimera that is stable with respect to perturbations is obtained. We have never seen its destruction even at very long simulations. Therefore, we can successively repeat the multiple chimera regeneration as long as computer power allows to process it. As the system complexity grows exponentially, we were only able to produce 4^n-rolled chimeras with $n = 1, 2, 3, 4$ and 5. Our largest example is the 1024-rolled chimera calculated for $N = 400$, i.e., for $N^3 = 64$ million oscillators up to 1000 time units, illustrated in Figure 4.

Stability regions for 4-, 16-, 64- and 256-headed parallel scroll wave chimera states are presented in Figure 5; the parameter point for the 1024-headed chimera from Figure 4 is also shown. As it can be observed, each next region in the cascade is twice thinner on the parameter r compared to the previous one. For instance, at

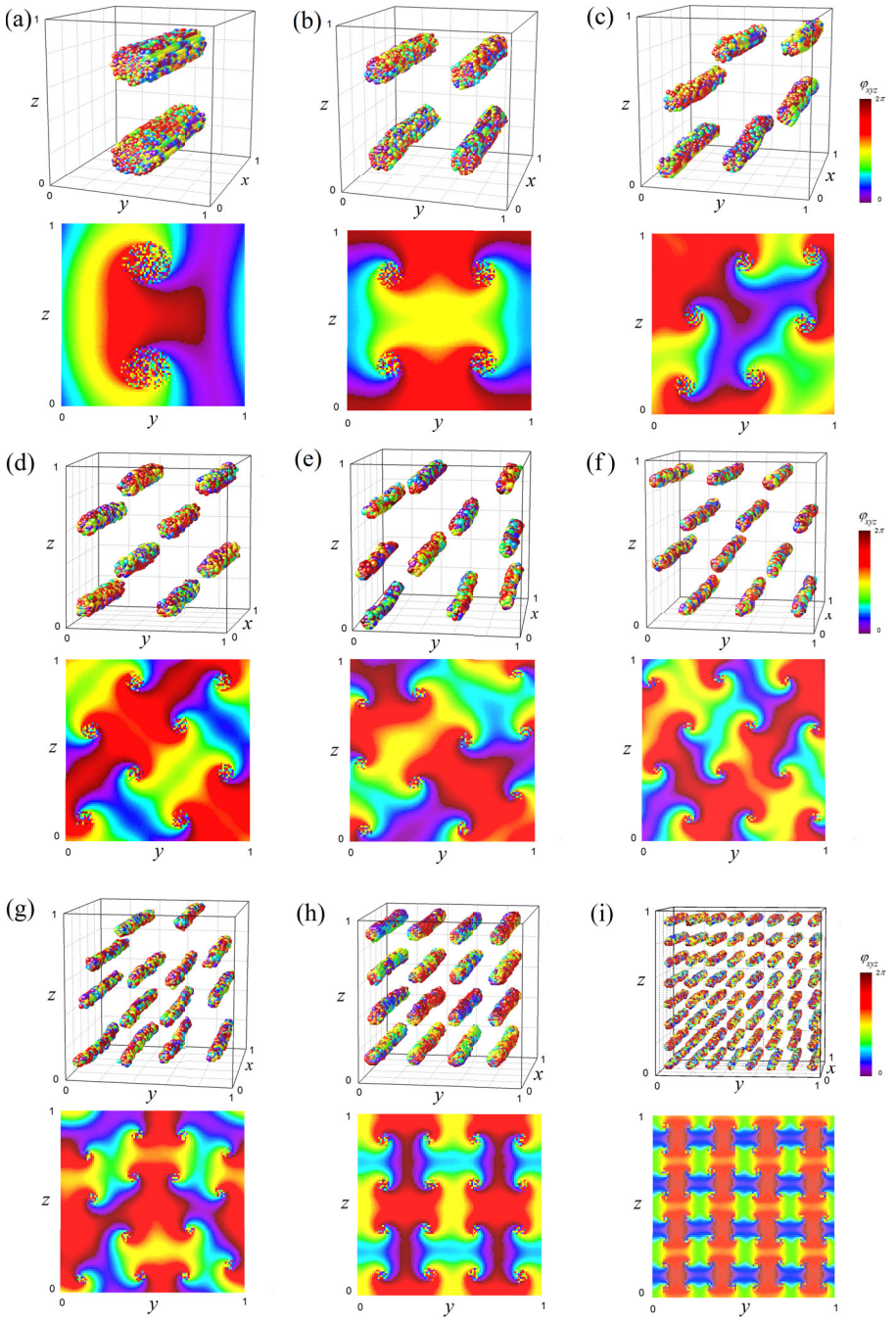

Fig. 2. Cascade of multiheaded scroll wave chimera states with parallel rolls. 3D screenshots and respective cross-sections are shown for: (a) two rolls ($\alpha = 0.8, r = 0.165$), (b) four rolls ($\alpha = 0.7, r = 0.12$), (c) 6 rolls ($\alpha = 0.7, r = 0.09$), (d) 8 rolls ($\alpha = 0.7, r = 0.08$), (e) 10 rolls ($\alpha = 0.64, r = 0.07$), (f) 12 rolls ($\alpha = 0.63, r = 0.05$), (g) 14 rolls ($\alpha = 0.64, r = 0.056$), (h) 16 rolls ($\alpha = 0.6, r = 0.06$), $N = 100$; (i) 64 rolls ($\alpha = 0.4, r = 0.04$). $N = 200$. Coordinates $x = i/N, y = j/N, z = k/N$.

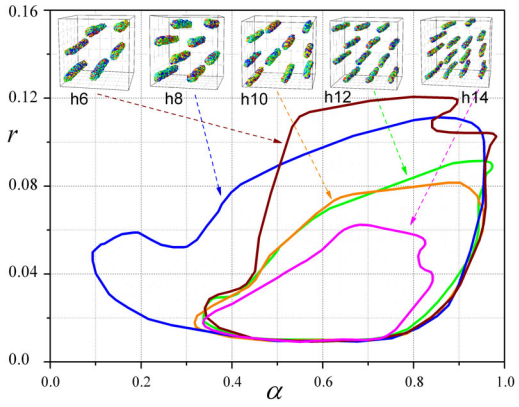

Fig. 3. Parameter regions for h-headed parallel rolls chimera states delineated by the color lines: blue – h6, brown – h8, orange – h10, green – h12, magenta – h14 rolls. $r = P/N, N = 100$. Snapshots of respective chimera types are shown in inserts.

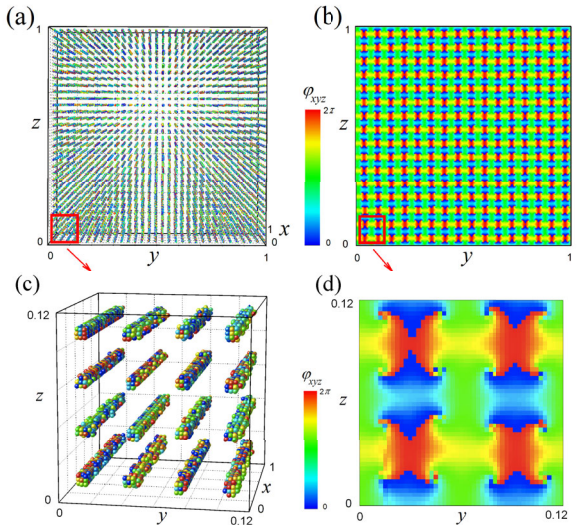

Fig. 4. Example of 1024-headed parallel scroll wave chimera state (a), and its cross-section at $x = 0.5$ (b) with enlarged windows (c,d) ($\alpha = 0.6, r = 0.0075, N = 400$).

$\alpha = 0.7$ the top border values of parameters r of the stability regions decreases approximately as 0.16, 0.08, 0.04, 0.02. We assume that with more computational power, the whole cascade can be obtained for the 4-multiple scroll wave chimeras with any $2^{2(n+1)}, n = 1, 2, 3...$ number of heads. Note that this cloning procedure can be also applied successfully for 4 crossed rolls chimera.

3 Hopf link and trefoil chimera states

Hopf link and trefoil chimera states represent 3D scroll waves with linked and knotted filaments. Due to the non-local coupling, the filaments are not singular (lines) as in standard scroll waves but "swelled" proportionally to the radius of coupling. Moreover, they are filled by oscillators with unsynchronized, chaotic behavior. The Kuramoto model, Hopf link and trefoil chimeras were fist reported in [13], see also [17]

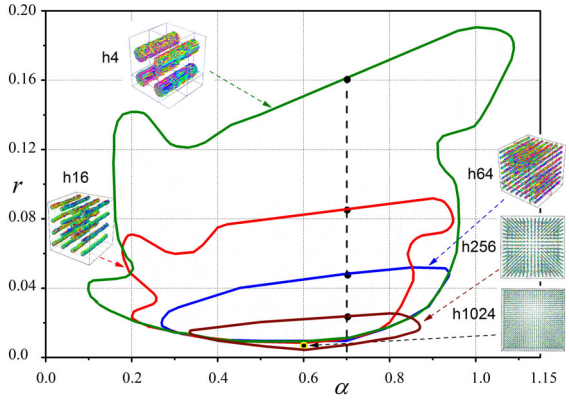

Fig. 5. Parameter regions for h-headed parallel rolled chimera states delineated by the color lines: olive – h4 ($N = 50$), red – h16 ($N = 100$), blue – h64 ($N = 100$), brown – h256 ($N = 200$) rolls. $r = P/N$. Snapshots of respective 3D chimera types are shown in inserts.

where bifurcation transitions between this kind of 3D patterns are studied for a different model with local coupling.

3.1 Cascades of multiple Hopf links and trefoils

In this section we design cascades of Hopf link and trefoil chimera states with additively growing the number of samples. Figures 6 and 7 illustrate the h-multiple cascades of Hopf links and trefoils, respectively, for $h = 1, 2, 3, \ldots, 8$ and 64. They are constructed by the cloning procedure using the the sampled initial conditions of identical Hopf links or trefoils, always with small perturbations to prevent the symmetry capturing. Constructed Hopf links and trefoils are not stationary patterns (in contrast to the parallel scroll waves in the previous section), this is illustrated by videos at `http://chimera3d.biomed.kiev.ua/multiheaded`.

We find that multiple chimera states of this kind exist in wide enough regions of the (α, r)-parameter plane. The regions are heavily intersecting and do not shrink as h increases. This is illustrated by the bifurcation diagrams in Figure 8 for $N = 200$. To our surprise, both parameter regions for single Hopf link and single trefoil coincide (delineated in black in Fig. 8). The same occurs for the respective multiple patterns. Indeed, 2-Hopf link and 2-trefoil states co-exist in the twice smaller region (delineated in blue). Moreover, the states of higher multiplicity $h = 3, 4, \ldots, 8$, are all found in the same slightly smaller inclusive region (delineated in green). Therefore, parameter regions for the h-multiple states stabilize as h increases and, given our precision, they become indistinguishable beginning from $h = 3$.

Regions for Hopf link and trefoil chimera states are located in the intermediate range of the phase lag parameter α, approximately between 0.6 and 0.9, and for rather small values of the coupling radius $r = P/N < 0.08$. The lower boundary of the regions is given by the value $r = 0.012245...$ ($N = 200$). This is the smallest value of r, when the number of nearest neighbors $\varphi_{i'j'k'}$ coupled to each oscillator φ_{ijk} is $N_{P_{min}} = 81$. At smaller $r < 0.012245$, the number of coupled oscillators drops abruptly to 59. Our simulations confirm that both single and multiple Hopf links and trefoils do not survive with such low connectivity ($P = 59$ or smaller) and are fast transforming into some other state. We conclude that Hopf links and trefoils arise in the Kuramoto model (1) only with non-local, prolonged coupling. Local diffusive coupling is not

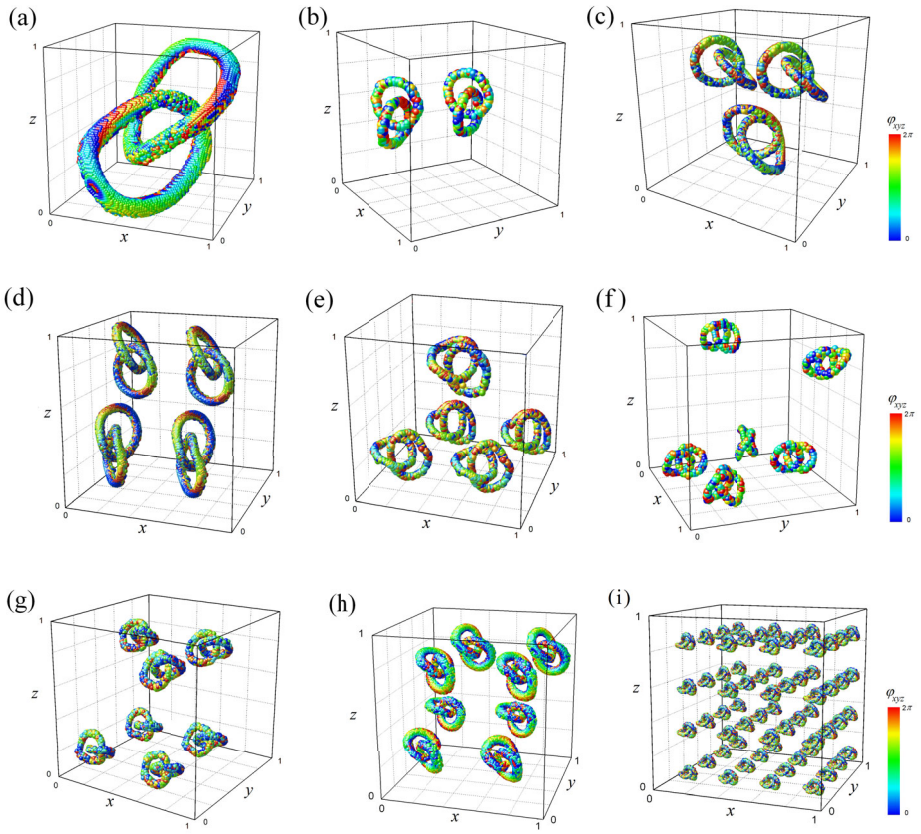

Fig. 6. Cascade of multiple Hopf link chimera states: (a) 1-headed ($\alpha = 0.76, r = 0.083, N = 100$), (b) 2-headed ($\alpha = 0.61, r = 0.0215$), (c) 3-headed ($\alpha = 0.61, r = 0.027$), (d) 4-headed ($\alpha = 0.68, r = 0.03$), (e) 5-headed ($\alpha = 0.68, r = 0.018$), (f) 6-headed ($\alpha = 0.7, r = 0.017$), (g) 7-headed ($\alpha = 0.74, r = 0.02$), (h) 8-headed ($\alpha = 0.84, r = 0.03$). $N = 200$; (i) 64-headed ($\alpha = 0.72, r = 0.01$), $N = 400$.

enough to insure their stability, which is unlike to the roll-type chimeras surviving at local coupling, see Section 2.

Multiple trefoil and Hopf link chimeras were obtained using the cloning procedure. It perfectly works, however, only when just 8 smaller copies of a state are laid into the unit cube. The other combinations, e.g., when looking for 2h, or 3h states, do not guarantee the desired result and require as a rule additional efforts. In many such cases the multi-compound structure appears to be unstable and is destroyed rather fast as simulations start. Then, we have to try again with different initial conditions and system parameters until the desired multi-headed Hopf link ot trefoil is eventually obtained.

3.2 Chain chimeras

For the single-link chimera two more kinds of linked scroll wave chimeras are given by single- and double-link chains, illustrated in Figure 9. In the R^3-cube the chains are broken, but they are indeed connected on the corresponding T^3-torus. Parameter regions for the chain chimeras are presented in Figure 10. As it can be seen, similar to the Hopf links and trefoils, they both arise in equation (1) at the intermediate values of the phase lag parameter α and for a rather small radius of coupling. For

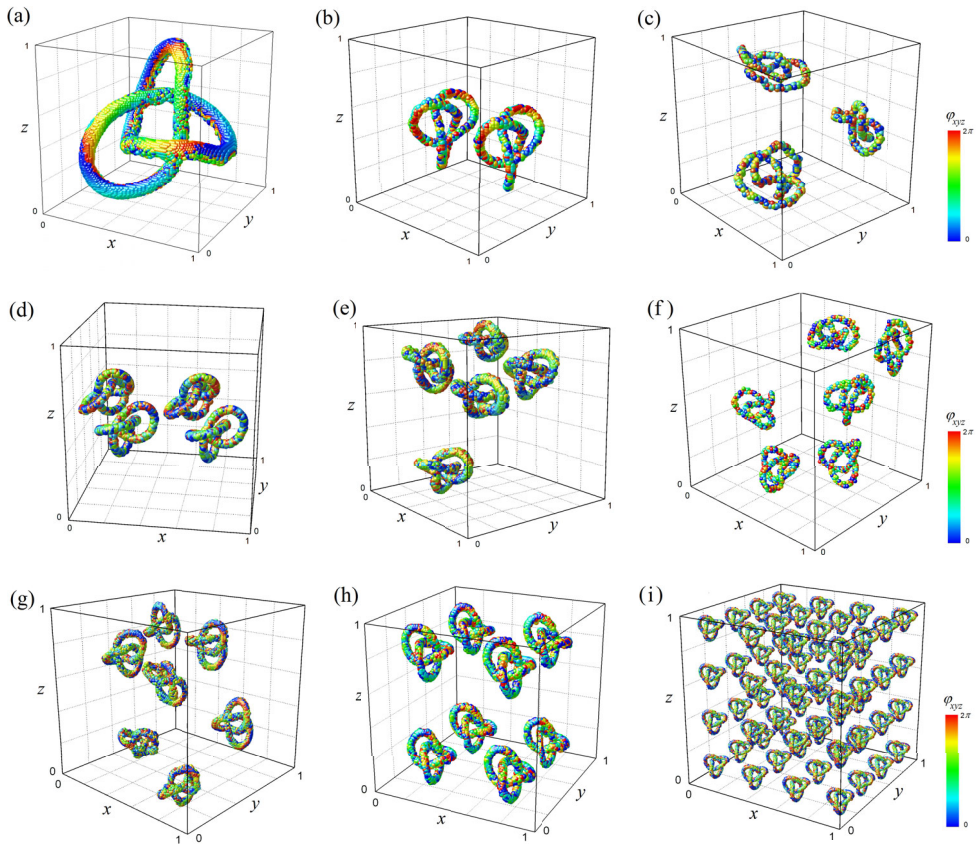

Fig. 7. Cascade of multiple trefoil chimeras states: (a) 1-headed ($\alpha = 0.68, r = 0.07, N = 100$); (b) 2-headed ($\alpha = 0.6, r = 0.023$), (c) 3-headed ($\alpha = 0.68, r = 0.02$), (d) 4-headed ($\alpha = 0.585, r = 0.02$), (e) 5-headed ($\alpha = 0.672, r = 0.02$), (f) 6-headed ($\alpha = 0.72, r = 0.02$), (g) 7-headed ($\alpha = 0.78, r = 0.02$), (h) 8-headed ($\alpha = 0.72, r = 0.02$), $N = 200$; (i) 64-headed ($\alpha = 0.72, r = 0.01$), $N = 400$.

single-link chains the parameter α should be approximately between 0.55 and 0.85, and r be smaller than 0.075.

The lower boundary of the single-link chain chimera is given by the coupling radius value $r = 0.00707...$ when each oscillator in the network is coupled to $N_P = 19$ of its nearest-neighbors. At smaller r the number N_P of the couplers drops abruptly to 7 only. The state becomes unstable and is rapidly destroyed in the simulations. Parameter regions in Figure 10 are obtained for equation (1) with $N = 200$. Interestingly, the same $N_P = 19$ lower bound on the number of coupled oscillators is also obtained for the chain chimera stability in equation (1) with $N = 100$.

Note that case of $N_P = 19$ couplers corresponds to the reliable numerical scheme for a PDE derived in [12], where 3D linked and knotted scroll waves have been obtained, however, only for a short time interval and their stability is not analyzed. Similarly, $N_P = 19$ in equation (1) can also be considered as local coupling. If so, we conclude that single-link chain chimera exist not only for the non-local but also for local coupling, and we expect that this can also be a robust pattern for the respective PDE in the limit $N \to \infty, r \to 0$. This situation is different from the Hopf link and trefoil stability, which have the pure non-local coupling origination (Sect. 3); on the other hand, it is similar to the rolls chimeras (scroll rings on T^3), see Section 2.

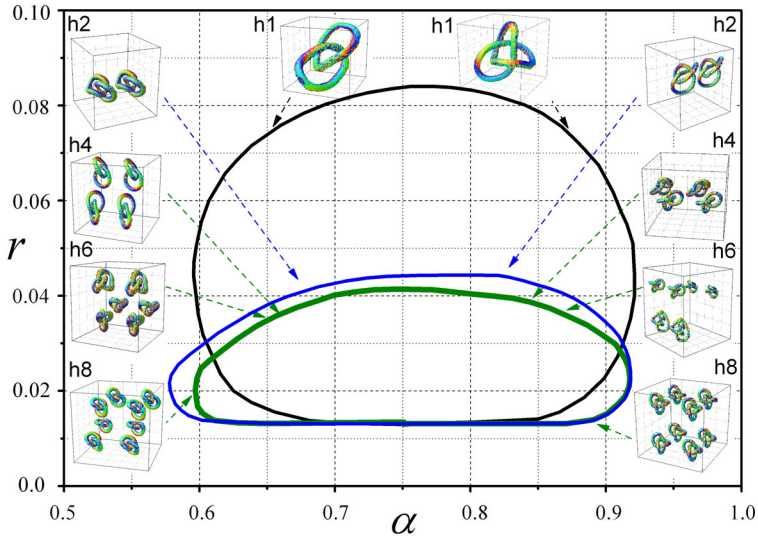

Fig. 8. Even cascades of Hopf link and trefoils: one-headed (delineated by black line), 2-headed (delineated by blue line), 4-headed, 6-headed and 8-headed (delineated by green line). $r = P/N, N = 200$. Snapshots of the chimera states are shown in inserts.

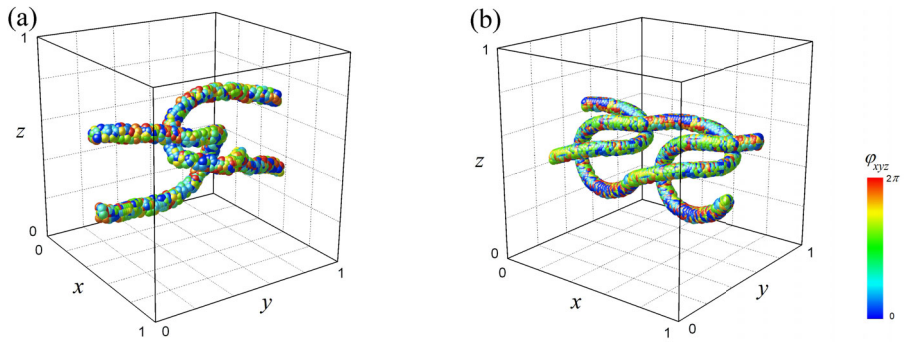

Fig. 9. Chain chimera states: (a) single-linked chain ($\alpha = 0.7, r = 0.041, N = 100$), (b) double-linked chain ($\alpha = 0.61, r = 0.033, N = 200$).

The double-link chain chimera exists in a smaller parameter region, see Figure 10, which is detached from the locally coupled case. Stability of the state begins with the non-locally coupling when $N_P = 27$ ($r = 0.01$ at $N = 200$). In our simulations, we have also tried to "clone" the chain chimeras with three and more links. However, they appear to be unstable and are rapidly destroyed in the presence of even very small perturbations.

3.3 Large-scale dynamics and transformations

Our simulations show that multiple Hopf link and trefoil chimera states often change their structure with time in the following way. When starting with 8 practically identical patterns placed in the unit cube, we observe soon afterwards that they group into 4 visibly different pairs, where the pairwise objects are only slightly different. To our surprise, without or with only tiny perturbations (10^{-4}) the pairwise identity appears to be so strong that it practically is not affected by the asymmetry of the Runge-Kutta numerical algorithm, and only imposed asymmetry in the initial conditions can

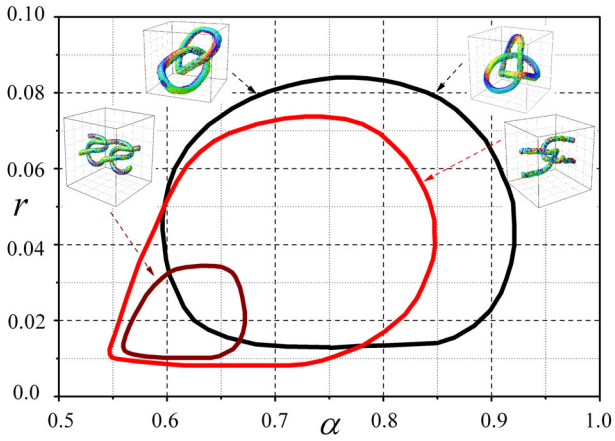

Fig. 10. Parameter regions for single-link (delineated by red line) and double-link (delineated by brown line) chain chimera states. Region for single Hopf link and trefoil are also shown (delineated by black line). $r = P/N, N = 200$.

slowly destroy it. On the other hand, each such pair in the chimera state has its own shape, size and position in the 3D space, distinct from the others. This is illustrated by the video at `http://chimera3d.biomed.kiev.ua/multiheaded/EvolutionT`.

Let us follow the dynamics of a multiheaded state inside the stability region shown in Figure 8. Take the 8-headed trefoil or Hopf links obtained from the single trefoil but with stronger perturbations of the initial conditions and start the simulations. Then, it is usually observed that in the some instants the samples collide and disappear or transform into other states. Eventually, as a rule, a hybrid state or a single-headed chimera is obtained.

Typical evolutions of a 8-headed trefoil and Hopf links chimera states with rather strong perturbations (0.1) of the identical initial conditions are demonstrated in the video at `http://chimera3d.biomed.kiev.ua/multiheaded/EvolutionS`. As one can observe there, the dynamics finally results in a single trefoil, Hopf link or other kinds of chimera states. It depends on the chosen initial cloning chimera, parameter values α, r and perturbation value. Usually the trajectory evolutions were calculated up to $t = 10^4$ for $N = 200$.

To obtained the odd-headed Hopf links and trefoils chimera, an odd number of initial chimeras should be taken in the cloning procedure and placed in the unit cube. Sometimes, as we have often seen in the simulations, odd-headed chimeras arise from strong enough perturbations of the even-headed ones. In all cases considered, the probability to obtain a desired odd-headed chimera was rather small, however after some number of trials, we could eventually catch it.

Twice repeating the 8-cloning procedure gives birth to 64-headed Hopf links and trefoils. As it is illustrated in Figure 6i and Figure 7i, each such pattern consist of 16 groups per 4 similar elements inside. Moreover, each 4 groups among the 16 are quite similar too. We expect that the head-adding sequence of the chimera states can be continued further, creating states with 512 and more objects. It requires, clearly, much more computational power to ensure the necessary accuracy of integrations. Indeed, the single Hopf link and trefoil states were obtained in our simulation of the N^3-dimensional network with $N = 100$; for the 8- and 64-headed states we had to take $N = 200$ and $N = 400$, respectively. In the latter case, a 64 million-dimensional nonlinear system should be integrated. The system complexity grows exponentially with further steps in the multiple chimera cascade.

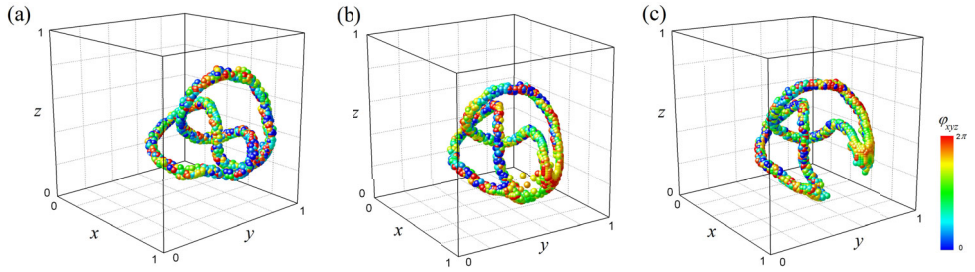

Fig. 11. Trefoil – Hopf link transformation: (a) trefoil ($t = 900$), (b) transformation beginning ($t = 990$), (c) Hopf link ($t = 1000$), $\alpha = 0.632, r = 0.04$, $N = 100$.

3.4 From trefoil to Hopf link

In our simulations, we often observed the situation when a trefoil chimera state transforms into a Hopf link (but not vise versa), see also [13,17]. The transition starts in the moment when trefoil branches touch each other. Soon afterwards the state transforms into a Hopf link or breaks down completely and disappears.

There are three ways for the trefoil→Hopf link transformation in equation (1). In the first case, when starting from random initial conditions, a trefoil is born, exists for some time interval, and then transforms into a Hopf link, see illustrative video at `http://chimera3d.biomed.kiev.ua/multiheaded/Hopflink`.

In the second case the trefoil→Hopf link transformation occurs as a result of a strong enough perturbation of the initial conditions (generated originally as a trefoil): `http://chimera3d.biomed.kiev.ua/multiheaded/evolution`. The third transformation scenario consists of the following: take a single trefoil inside its stability region, see Figure 8, and move the parameter point to the boundary. When close to the boundary, it is often observed that the trefoil can suddenly transform into a Hopf link.

To illustrate the latter scenario, fix parameters $\alpha = 0.6325, r = 0.04$ close to the boundary of the trefoil stability region. Shift the parameter α to 0.632 and start simulations. At $t = 900$ the trefoil still exists (Fig. 11a) but soon after, at $t = 990$ two trefoil branches touch each other, and the transformation to a Hopf link begins (in Fig. 11b). At $t = 1000$ (Fig. 11c) a Hopf link is created, and it persists for long in continuing simulations.

4 Hybrid scroll wave chimeras

In the previous sections, different multiheaded scroll wave chimera states were reported for equation (1), each including similar incoherent elements such as rolls, Hopf links, trefoils, or chains only. Here, we demonstrate a possibility of hybrid-type organization for the multiheaded chimera states which can combine different of the above mentioned single-headed chimera types.

To obtain hybrid-type scroll wave chimeras we have tested different sample combinations in the cloning procedure. There is no guarantee that the process will be successful. In many trials the cloned hybrid-type chimeras get destroyed very fast, and the procedure has to be repeated starting from a different number organization of the initial 'chimera clones', also varying the parameters and the magnitude of the perturbations.

Screenshots of characteristic hybrid-type scroll wave chimera states with additively growing number of samples are presented in Figure 12 such as: (a) Hopf link and

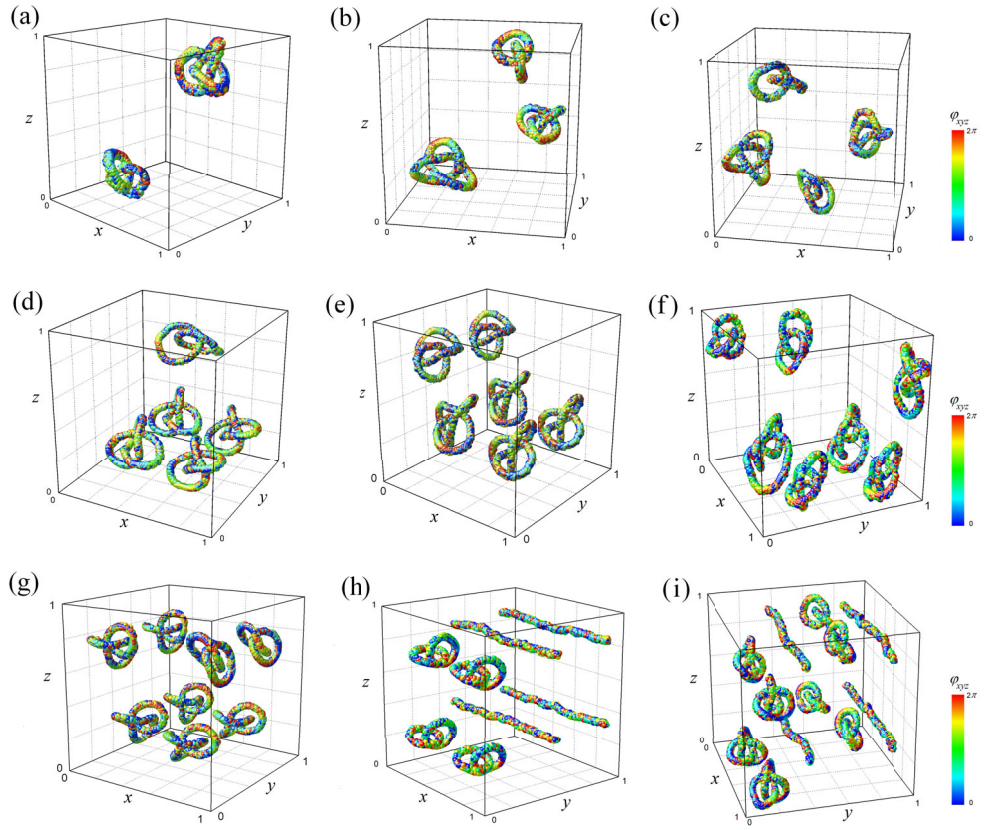

Fig. 12. Examples of multiheaded hybrid chimera states: (a) one trefoil and one Hopf links ($\alpha = 0.785, r = 0.02$), (b) 2 trefoils and one Hopf links ($\alpha = 0.755, r = 0.02$), (c) 2 trefoils and 2 Hopf links ($\alpha = 0.735, r = 0.02$), (d) 4 trefoils and one Hopf links ($\alpha = 0.625, r = 0.02$), (e) 4 trefoils and 2 Hopf links ($\alpha = 0.615, r = 0.02$), (f) 5 trefoils and 2 Hopf links ($\alpha = 0.68, r = 0.02$), (g) 6 trefoils and 2 Hopf links ($\alpha = 0.64, r = 0.02$), (h) 4 Hopf links and 4 scroll wave rolls ($\alpha = 0.7, r = 0.02$). (i) 4 Hopf links, 4 trefoils and 4 scroll wave rolls ($\alpha = 0.76, r = 0.02$). $N = 200$.

trefoil, (b) Hopf link and 2 trefoils, (c) 2 Hopf links and 2 trefoils, (d) Hopf link and 4 trefoils, (e) 2 Hopf links and 4 trefoils, (f) 2 Hopf links and 5 trefoils, (g) 2 Hopf links and 6 trefoils, (h) 4 Hopf links and 4 rolls ($\alpha = 0.7, r = 0.02$), (i) 4 Hopf links, 4 trefoils and 4 rolls.

These states exist for long times, up to $t = 10^4$ at least. They are non-stationary objects in 3D and are usually characterized by the non-trivial temporal large-scale dynamics. In our simulations we have also observed some other hybrid patterns, also preserving for long-time simulations.

See videos at `http://chimera3d.biomed.kiev.ua/multiheaded/hybrid`, where more examples of the hybrid-type chimeras are shown.

To finalize, our last example is a 80-headed scroll wave chimera state including 32 Hopf links, 32 trefoils, and 16 rolls illustrated in Figure 13. The state is calculated for N = 400 (i.e., 64 million oscillators), simulation time was $t = 1000$.

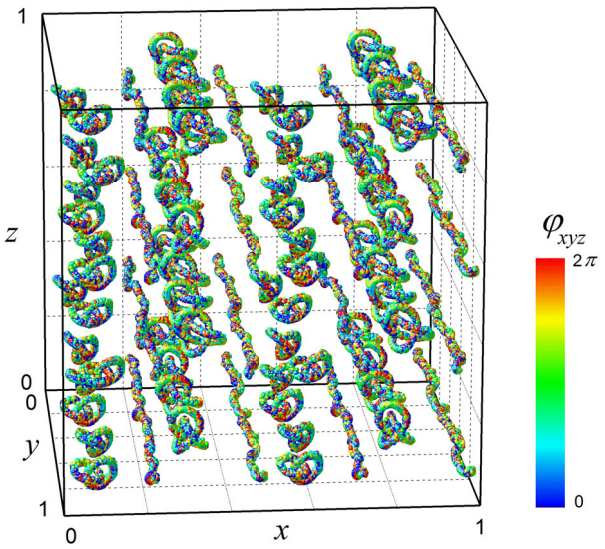

Fig. 13. Example of 80-headed hybrid chimera state consisting of 32 trefoils, 32 Hopf links, and 16 rolls ($\alpha = 0.76, r = 0.01$). $N = 400$.

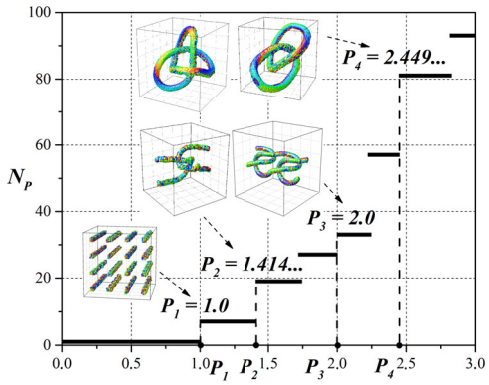

Fig. 14. Number of oscillators N_P coupled to each oscillator in the model (1) depending on the value of $P = rN$. Parallel and crossed rolled chimeras exist beginning from $P = P_1 = 1.0$ ($N_P = 7$), single-link chains – from $P = P_2 = 1.414\ldots$ ($N_P = 19$), double-link chains – from $P = P_3 = 2.0$ ($N_P = 27$), trefoils and Hopf links – from $P = P_4 = 2.44948\ldots$ ($N_P = 81$). The minimal values N_P are found to be the same for $N = 100, 200$, and 400.

5 Conclusion

We have demonstrated a diversity of multiple scroll wave chimeras for the three-dimensional network of coupled Kuramoto phase oscillators with non-local coupling. Wide parameter regions are obtained for rolls, chains, Hopf links, and trefoil patterns. It follows, in particular, that rolled chimeras exist not only for non-local but also for local coupling schemes, beginning from only $N_P = 7$ nearest-neighbor couplers (as in the simplest diffusive coupling scheme). This fact is schematically indicated by the left corner inset in Figure 14.

The next chimera state to appear when increasing the coupling radius $r = N/P$ in equation (1) is the single-link chain, this occurs in the case of $N_P = 19$ couplers. At further increase of the coupling radius r, first, the double-link chain stabilizes

for $N_P = 27$ couplers ($r = 0.01$ at $N = 200$). Then, only at $N_P = 81$ ($r = 0.02449$) a variety in single and multiple Hopf links and trefoils become stable to exist further for this and larger values of r, up to appr. 0.08.

An essential condition for the scroll wave chimeras appearance is the intermediate value of the phase shift α, appr. between 0.6 and 0.9. Therefore, Hopf link and trefoil chimera states exist in the Kuramoto model only with essentially non-local coupling and sufficiently large phase shift. On the other hand, multiple rolled chimeras which are actually the scroll rings in the circular coordinates are more stable objects. They grow not only for non-local but even for local, diffusive-type coupling schemes. Single-link chain chimeras are also preserved in the locally coupling case, but not the double-link ones which require some level of non-locality for the stabilization. We believe that the described fascinating scroll wave chimeras can be found in other, more realistic 3D networks displaying one of the inherent features of nature, that is due to non-local coupling.

We thank B. Fiedler, E. Knobloch, P. Manneville and M. Hasler for illuminating discussions, and the Ukrainian Grid Infrastructure for providing the computing cluster resources and the parallel and distributed software.

References

1. Y. Kuramoto, D. Battogtokh, Nonlinear Phenom. Complex Syst **5**, 380 (2002)
2. D.M.Abrams, S.H. Strogatz, Phys. Rev. Lett. **93**, 174102 (2004)
3. M.J. Panaggio, D.M. Abrams, Nonlinearity **28**, R67 (2015)
4. E. Schöll, Eur. Phys. J. Special Topics **225**, 891 (2016)
5. Y. Kuramoto, S.I. Shima, Prog. Theor. Phys. Supp **150**, 115 (2003)
6. S.I. Shima, Y. Kuramoto, Phys. Rev. E **69**, 036213 (2004)
7. P.-J. Kim, T.-W. Ko, H. Jeong, H.-T. Moon, Phys. Rev. E **70**, 065201(R) (2004)
8. E. Martens, C. Laing, S. Strogatz, Phys. Rev. Lett. **104**, 044101, (2010)
9. O. Omel'chenko, M. Wolfrum, S. Yanchuk, Yu. Maistrenko, O. Sudakov, Phys. Rev. E **85**, 036210 (2012)
10. M.J. Panaggio, D.M.Abrams, Phys. Rev. Lett. **110**, 094102 (2013)
11. J. Xie, E. Knobloch, H.-C. Kao, Phys. Rev. E **92**, 042921 (2015)
12. Yu. Maistrenko, O. Sudakov, O. Osiv, V. Maistrenko, New J. Phys. **17**, 073037 (2015)
13. H.W. Lau, J. Davidsen, Phys. Rev. E **94**, 010204(R) (2016)
14. Yu. Maistrenko, A. Vasylenko, O. Sudakov, R. Levchenko, V. Maistrenko, Int. J. Bifurc. Chaos **24**, 1440014 (2014)
15. A. Salnikov, R. Levchenko, O. Sudakov, in *Proc. 6-th IEEE Workshop IDAACS'2011* (2011), pp. 198–202
16. M. Zynovyev, M. Svistunov, O. Sudakov, Yu. Boyko, in *Proc. 4-th IEEE Workshop IDAACS'2007* (2007), pp. 165–169
17. B. Fiedler, R. Mantel, Dokumenta Mathematica **5**, 695 (2000)